Check for updates
Natural Product Sciences
30(3) : 212-219 (2024)
https://doi.org/10.20307/nps.2024.30.3.212

Methylene Chloride Fraction of *Saururus chinensis* Inhibits Adipocyte Differentiation in 3T3-L1 Cells and Reduces Lipid Accumulation in High-Fat Diet-Fed C57BL/6 Mice

Jaemoo Chun[1,†,*], Bo Eun Kim[2,†], Mibae Jeong[1], and Yeong Shik Kim[2,*]

[1]*KM Convergence Research Division, Korea Institute of Oriental Medicine, Daejeon 34054, Republic of Korea*
[2]*Natural Products Research Institute, College of Pharmacy, Seoul National University, Seoul 08826, Republic of Korea*

Abstract – The aerial parts of *Saururus chinensis* (Lour.) Baill., known for its rich lignan content and diverse pharmacological activities such as anti-inflammatory and anticancer effects, has not been extensively explored for its potential in preventing obesity. In this study, we investigated the inhibitory effect of methylene chloride fraction of *S. chinensis* (MCSC) on adipocyte differentiation using experimental models. Furthermore, we conducted a comprehensive chemical analysis employing HPLC and LC-ESI/MS to identify and characterize the main compounds responsible for these effects. MCSC significantly inhibited preadipocyte differentiation, accompanied by down-regulation of target genes involved in lipid synthesis and storage. This anti-adipogenic effect was mediated by the inhibition of CCAAT/enhancer binding protein α (C/EBPα) and peroxisome proliferator-activated receptor γ (PPARγ) expression. In a mouse model, oral administration of MCSC resulted in reduced body weight and adipose tissue weight, along with improvements in serum lipid profiles in high-fat diet-induced C57BL/6 obese mice. Active ingredients were identified as manassantin A and manassantin B through comparison of their spectrometric features with previously reported data. This evidence suggests that MCSC could be a potential candidate for the treatment and prevention of obesity-associated diseases.

Keywords – *Saururus chinensis*, Lignan, Anti-adipogenic effect, Anti-obesity, C/EBPα, PPARγ

Introduction

Obesity has become a pervasive health concern, with its incidence steadily increasing.[1] It is associated with significant health risks, including cardiovascular disease, type II diabetes, and non-alcoholic fatty liver disease.[2] Despite the urgency of addressing obesity, current anti-obesity therapies are limited. Conventional approaches involve either inhibiting fat absorption to suppress lipid breakdown in the intestine or reducing appetite through modulation of the central nervous system.[3–5]

Adipogenesis is a differentiation process that occurs in response to the need for additional fat mass stores in the form of triglycerides, which increases when caloric intake exceeds nutritional requirements.[6] Adipose tissue growth is associated with the formation of new adipocytes from precursor cells and an increase in adipocyte size.[7] The expansion of adipose tissue involves both an increased number of adipocytes (hyperplasia) due to the enhanced differentiation of preadipocytes into adipocytes, and an increased size of adipocytes (hypertrophy) due to lipid accumulation.[8,9] Regulating the adipocyte life cycle and controlling adipocyte size and number offer promising therapeutic avenues for obesity management.[10,11] During the stage of adipocyte differentiation, CCAAT/enhancer binding protein α (C/EBPα) and peroxisome proliferator-activated receptor γ (PPARγ), which are two major adipogenic transcription factors, regulate the lipid homeostasis by controlling the expression of target genes, including fatty acid synthase (FAS), adipocyte fatty acid binding protein 4 (aP2), sterol regulatory element binding protein-1 (SREBP-1), and stearoyl-CoA desaturase-1 (SCD-1), all of which are associated with fat accumulation by these transcription factors.[12,13]

Saururus chinensis (Lour.) Baill (Saururaceae) has been used as a traditional medicine in Korea for treating various diseases, such as edema, gonorrhea, jaundice, and inflammatory diseases.[14–16] Previous reports have shown that *S. chinensis* exhibits antioxidant,[17] anti-inflammatory,[18] anticancer,[19] and anti-obesity effects.[20] Although the inhibitory effect of *Saururus chinensis* on

*Author for correspondence
Jaemoo Chun, Ph. D., KM Convergence Research Division, Korea Institute of Oriental Medicine, Daejeon 34054, Republic of Korea
Tel: +82-42-868-9511; E-mail: jchun@kiom.re.kr
Yeong Shik Kim, Ph. D., Natural Products Research Institute, College of Pharmacy, Seoul National University, Seoul 08826, Republic of Korea
※ 개인정보 표시제한 E-mail: kims@snu.ac.kr
[†]These authors contributed equally to this work.

adipogenesis has been reported in 3T3-L1 adipocytes, a systemic study on the efficacy of its fractions, including *in vivo* experiment, has not been conducted. In this study, we investigated the effect of *S. chinensis* on adipocyte differentiation and the expression of adipogenic genes both *in vitro* and *in vivo*. Furthermore, we identified the anti-obesity phytochemicals in *S. chinensis* using chromatography techniques.

Experimental

General experimental procedures – Dulbecco's modified Eagle's medium (DMEM), penicillin, streptomycin, and fetal bovine serum (FBS) were obtained from GenDepot (Barker, TX, USA). 3-(4,5-dimethylthiazol-2-yl)-2,5-diphenyltetrazolium bromide (MTT) and Oil-Red O were purchased from Sigma Aldrich (St. Louis, MO, USA). Antibodies against PPARγ, C/EBPα, and β-actin were purchased from Santa Cruz Biotechnology (Santa Cruz, CA, USA). All organic solvents used for extraction and column chromatography were purchased from Duksan Chemical Co. (Seoul, Korea). HPLC-grade acetonitrile and methanol used for HPLC analysis and LC-ESI/MS were obtained from J.T. Baker (Philipsburg, NJ, USA).

Preparation of plant extract and fractions – The dried aerial parts of *S. chinensis* were purchased from Omni Herbs (Seoul, Korea) and identified by Professor Youngbae Suh of Seoul National University. A voucher specimen (NPRI-11-726) was deposited at the Herbarium of the Natural Products Research Institute at Seoul National University. The aerial parts of *S. chinensis* (1.5 kg) were extracted three times with 6 L of 70% methanol for 1 h by sonication. The extract was then filtered and evaporated under reduced pressure to obtain a crude extract (272.2g). The extract was suspended in distilled water and sequentially partitioned with *n*-hexane, methylene chloride, ethyl acetate, and *n*-butanol three times to yield *n*-hexane fraction (10.7 g), methylene chloride fraction (7.4 g), ethyl acetate fraction (7.0 g), and *n*-butanol fraction (17.9 g), respectively. The scheme of sample preparation was outlined in Fig. 1A.

Cell culture – Mouse 3T3-L1 fibroblast cells were obtained from the American Type Culture Collection (Manassas, VA, USA). 3T3-L1 preadipocytes were grown in DMEM supplemented with 10% bovine calf serum, 25 mM HEPES, penicillin (100 units/mL), and streptomycin (100 μg/mL) until confluent at 37°C in a humidified atmosphere containing 5% CO_2. Two days after confluency, preadipocytes were differentiate with DMEM supplemented with 10% FBS and the differentiation inducer (MDI): 0.5 mM isobutylmethylxanthine, 1 μM dexamethasone, and 10 μg/mL insulin for 2 days. Cells were then maintained in DMEM supplemented with 10% FBS and 10 μg/mL insulin for 2 days, followed by culturing with DMEM supplemented with 10% FBS medium for an additional 4 days. At this time, more than 90% of the cells were mature adipocytes with accumulated lipid droplets.

Cell viability assay – Cell viability was determined using an MTT assay. 3T3-L1 cells were seeded into a 96-well plate and treated with various concentrations of samples for 48 h. The MTT solution (0.5 mg/mL) was added to each well and the absorbance was measured at a wavelength of 595 nm using a microplate reader (Molecular Devices, Sunnyvale, CA, USA).

Oil-Red O staining – Differentiated adipocytes were stained with Oil-Red O on day 8. The cells were fixed in 4% formaldehyde, stained with 0.5% Oil-Red O solution for 2 h, and observed under a Leica microscope at 400× magnification. For the quantification, the stained cells were solubilized with 4% NP-40 and measured at a wavelength of 490 nm using a microplate reader.

Western blotting – 3T3-L1 cells and animal tissues were extracted with cell lysis buffer containing 20 mM Tris-Cl (pH 7.5), 150 mM NaCl, 1 mM Na_2EDTA, 1 mM EGTA, 1% NP-40, 1% sodium deoxycholate, 2.5 mM sodium pyrophosphate, 1 mM Na_3VO_4, 1 mM DTT, 1 mM PMSF, and a protease inhibitor cocktail. Equal amounts of protein were separated on a 10% SDS-PAGE and transferred to a nitrocellulose membrane. The membrane was blocked with 5% bovine serum albumin and incubated with primary antibodies followed by corresponding secondary antibodies conjugated with horseradish peroxidase. The immunoreactive bands were developed using a chemiluminescence kit (AB Frontier, Seoul, Korea) and visualized using a LAS-1000 image analyzer (Fujifilm, Tokyo, Japan).

Quantitative reverse transcription (qRT)-PCR – Total RNA was extracted from cells, homogenized livers, and adipose tissues using a Trizol reagent kit (Invitrogen, Carlsbad, CA, USA). 1 μg of RNA was converted to cDNA with the iScript™ Select cDNA Synthesis Kit (Bio-Rad, Hercules, CA, USA). qRT-PCR was performed with a 7300 Real-Time PCR system (Applied Biosystems, Carlsbad, CA, USA) using SYBR Green PCR Master Mix Kit (Bio-Rad). Predesigned Quantitect primers aP2 (NM_024406), FAS (NM_007988), SREBP1 (NM_011480), SCD1 (NM_009127), and GAPDH (NM_008084) were obtained from Qiagen (Valencia, CA, USA). Relative gene expression was evaluated by the comparative Ct method and normalized using GAPDH.

Animal experiments – Animal care and all the procedures were conducted according to the guidelines of Seoul National

University Institutional Animal Care and Use Committees (SNU-120102-6). Male C57BL/6 mice at the age of 5 weeks were purchased from Central Animal Laboratory (Seoul, Korea) and acclimated for one week before experimental use. The mice were housed under the following environmental conditions (temperature 22°C; humidity 50%; 12 h light/dark cycle). Normal mice were fed a standard chow diet (Samyang, Seoul, Korea) and given free access to drinking water. To generate high-fat diet (HFD)-induced obesity, mice were fed an HFD (D-12492, Research Diets, New Brunswick, NJ, USA) for 6 weeks. HFD-fed mice were randomly divided into 3 groups ($n = 8$) as follows: mice only fed an HFD, mice fed an HFD with MCSC (15 mg/kg/day and 30 mg/kg/day, orally). The mice were fed and watered *ad libitum* for 14 weeks. The body weight and food consumption were recorded once a week and twice a week, respectively.

Serum analysis – Blood was collected at the end of the experiment for biochemical analysis in fasted mice. Serum samples were obtained by centrifuging the fresh blood for 20 min at 6,000 rpm at 4°C. Alanine aminotransferase (ALT), aspartate aminotransferase (AST), triglycerides, total cholesterol, and glucose levels were measured using a commercial enzyme kit (Asan Pharmaceutical Co, Seoul, Korea).

Histological analysis – The liver and adipose tissues were fixed in 10% formaldehyde, dehydrated, and embedded in paraffin wax. Cross-sections were cut at 4 μm and stained with hematoxylin and eosin (H&E) and Oil-Red O solution. The sections were viewed and photographed with a Leica microscopy.

Bioactivity-guided identification of compounds – The HPLC analysis was carried out on a Hitachi L-6200 instrument equipped with a UV detector system and a SIL-9A auto-injector (Shimadzu, Japan). Methylene chloride fraction was subjected to column chromatography over silica gel (Silica gel 60; 0.063–0.200 mm, MERCK) eluted with *n*-hexane-acetone (7:1, 5:1, 3:1, 1:1, 1:3, 1:5, *v*/*v*) to afford 6 fractions (F1–F6). F4 (1.1 g) was further applied to a silica gel column chromatography (3.5 × 40 cm) eluting with ethyl acetate-methanol-water (100:10:5, *v*/*v*), affording 15 fractions (F4.1–F4.15). F4.3 was sub-fractionated using an MPLC system. Chromatographic separation of compounds was performed using a Zorbax SB-Aq C_{18} column (75 mm × 2.3 mm i.d., 3.5 μm) from Agilent Technologies (Palo Alto, CA, USA) using a mobile phase composed of differing proportions of 0.1% formic acid in water (solvent A) and 0.1% formic acid in acetonitrile (solvent B). The samples were eluted with the gradient 0–10 min (40–70% B), 10–15 min (70–100% B), washing with 100% B and 40% B at a flow rate of 0.2 mL/min. Liquid chromatography with tandem mass spectrometry detection was performed on an Agilent 1100 HPLC system and a Thermo Finnigan LQD Deca (San Jose, CA), equipped with an electrospray ion source. Compounds were identified by an Agilent 6530 Accurate-Mass QTOF LC/MS. All ion trap analyzer parameters were optimized according to the manufacturer's instructions. The following optimized MS condition were selected: a sheath gas flow of 70 arbitrary units, a capillary temperature of 275°C, a capillary voltage of -10kV, source fragmentation energy 25%, and a spray voltage of 4.5 kV in negative mode.

Statistical analysis – All the data are presented as the mean ± standard deviations (SD). Student's *t*-test and analysis of variance with Dunnett's post hoc test were used for the statistical analysis of multiple comparisons. A value of $p < 0.05$ was considered statistically significant.

Results and Discussion

The extract of *S. chinensis* is known to exhibit hypolipidemic, hypoglycemic, lipid-lowering, and hepatoprotective effects.[21,22] Although several anti-adipogenic properties of *S. chinensis* have been reported, there is limited evidence regarding the fractions and components of *S. chinensis* on lipogenesis in adipocytes and adipose tissues. We investigated the effects of methanol extract of *S. chinensis* (MESC) and each fraction on lipid accumulation in 3T3-L1 cells. The lipid accumulation of MESC and its five solvent fractions was evaluated by Oil-Red O staining. As shown in Fig. 1B, MESC significantly suppressed lipid accumulation in a dose-dependent manner. However, MESC treatment up to 5.0 μg/mL had no effect on the cell viability of 3T3-L1 cells. Furthermore, we confirmed that hexane, methylene chloride, and ethyl acetate fractions decreased lipid accumulation without affecting cell viability. Among these fractions, methylene chloride fraction of *S. chinensis* (MCSC) potently inhibited lipid accumulation in 3T3-L1 cells. Although hexane and ethyl acetate fractions showed an inhibitory effect on lipid accumulation, MCSC exhibited the strongest effect. In particular, it demonstrated strong inhibitory effect even at a low concentration of 0.2 μg/mL, whereas other fractions did not. Therefore, we speculated that MCSC contains significant amounts of active substances and set the concentrations of MCSC to 0.1, 0.25, and 1.25 μg/mL in the following study.

We investigated the inhibitory effect of MCSC on 3T3-L1 adipocyte differentiation. We initially examined the cytotoxicity of MCSC in 3T3-L1 cells. As shown in Fig. 2A, MCSC treatment up to 2.5 μg/mL had no adverse effect on the cell viability of 3T3-L1 cells. To further explore the anti-obesity effect of MCSC on adipocyte differentiation, 3T3-L1 cells were differentiated

with MDI complex (isobutylmethylxanthine, dexamethasone, and insulin) in the absence or presence of MCSC. MCSC treatment dose-dependently decreased lipid accumulation in 3T3-L1 adipocytes (Fig. 2B, C), suggesting that MCSC may possess potential anti-obesity properties by inhibiting adipocyte differentiation.

Critical adipogenic transcription factors, C/EBPα and PPARγ, play pivotal roles in the early stages of adipocyte differentiation, promoting the expression of genes involved in lipid biosynthesis and storage.[23] To investigate whether MCSC regulates adipogenesis through C/EBPα and PPARγ, we assessed the protein expression using western blotting. The expression of C/EBPα and PPARγ in 3T3-L1 cells was upregulated by MDI treatment. However, MCSC treatment significantly inhibited the protein expressions of C/EBPα and PPARγ in a dose-dependent manner (Fig. 3A, B). Furthermore, the mRNA levels of aP2, FAS, SREBP-1, and SCD1 were confirmed by qRT-PCR. The results showed that MCSC decreased the mRNA expression of aP2 which is downstream of PPARγ, FAS involved in the fatty acid synthesis, SREBP-1, and SCD-1 in a dose-dependent manner (Fig. 3C). The observed down-regulation of C/EBPα and PPARγ aligns with reduced mRNA levels of their downstream targets such as aP2, FAS, SREBP-1, and SCD1. These results suggest that MCSC interferes with the adipogenic signaling pathway, thereby inhibiting the conversion of preadipocytes to mature adipocytes.

To investigate whether MCSC could modulate obesity in animal models, we used HFD-induced obese mouse. Mice with diet-induced obesity were orally administered with 15 and 30 mg/kg MCSC for 8 weeks. The results showed that MCSC has a weight-lowering effect in HFD-induced obese mice (Fig. 4A). The reduced body weight gain in the MCSC-administered mice group was related to decreased fat accumulation. As shown in Fig. 4B, the weight of adipose tissue was distinctly reduced in the MCSC 30 mg/kg-treated group, showing that the alleviated obesity in MCSC-treated mice is due to the reduced adiposity in the abdominal adipose tissues. Although there was no significant difference in the weight of liver between the ND and HFD groups at 14 weeks, the MCSC 30 mg/kg-treated group showed a decrease in the weight of liver, compared to the HFD group (Fig. 4C). Next, we collected the blood samples to observe the biochemical changes within serum. This weight reduction was associated with an improvement in serum lipid profiles, including lowered levels of ALT, AST, glucose, triglycerides, and total cholesterol, indicating a positive impact on metabolic health. As shown in Fig. 4D, elevated concentrations of ALT and AST were confirmed in the HFD group compared to normal diet group. However, a significant reduction in the concentrations of ALT and AST was observed in MCSC groups compared to the HFD group. To examine changes in serum levels of lipid metabolism markers, the levels of fasting glucose, triglycerides, and total cholesterol were evaluated. The HFD group showed a notable increase in concentrations of glucose, triglycerides, and total cholesterol compared to the normal diet group. However, the MCSC groups showed a significant decrease in levels of these markers, compared to the HFD group.

The hepatic accumulation of lipids and hypertrophic adipocytes was investigated by pathological analysis of sections

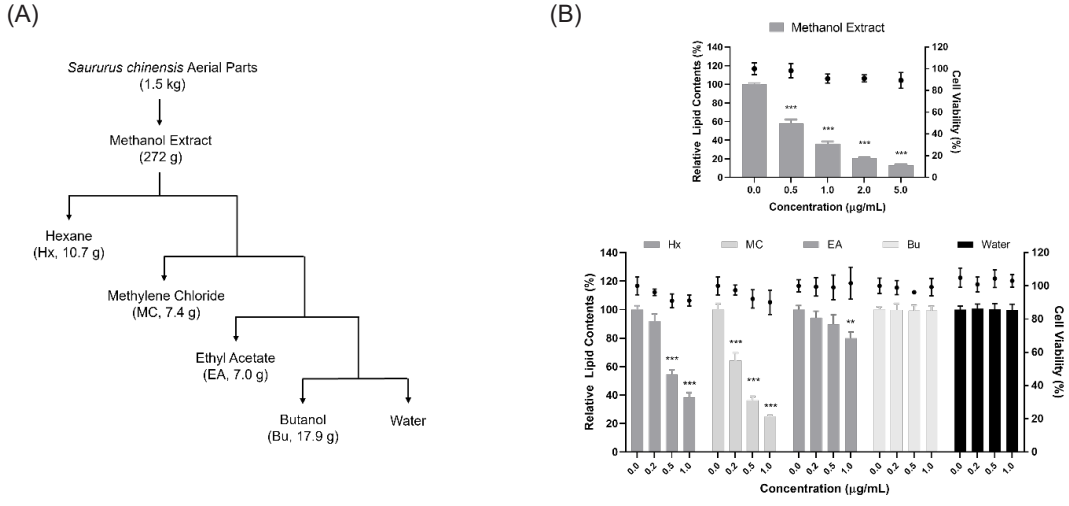

Fig. 1. (A) Scheme of bioassay-guided fractionation. (B) Inhibitory effect of methanol extract of *Saururus chinensis* (MESC) and its fractions on lipid accumulation in 3T3-L1 cells. 3T3-L1 cells were treated with MESC (0.5–5 μg/mL) and its fractions (0.2–1 μg/mL). Lipid droplets accumulated in cells were stained with Oil-Red O on day 8 after the induction of differentiation. Cell viability was evaluated by MTT assay. The results are presented as the mean ± SD of three independent experiments. ***$p < 0.001$ indicates the significance compared to control group.

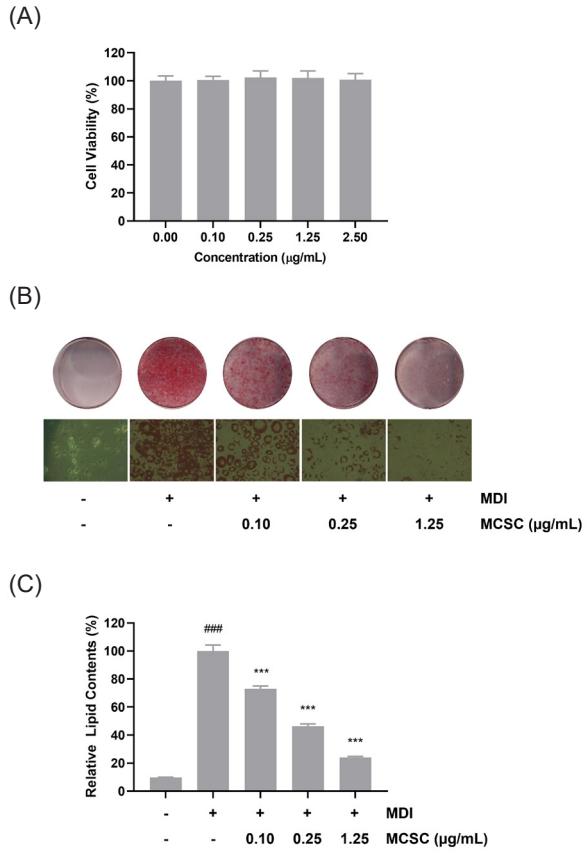

Fig. 2. Inhibitory effect of methylene chloride fraction of *S. chinensis* (MCSC) on 3T3-L1 adipocyte differentiation. (A) The effect of MCSC on cell proliferation in 3T3-L1 cells. (B) Inhibitory effect of MCSC on lipid accumulation in 3T3-L1 cells. 3T3-L1 cells were differentiated with MDI complex (isobutylmethylxanthine, dexamethasone, and insulin) in the absence or presence of MCSC for 8 days. Lipid droplets accumulated in cells were stained with Oil-Red O on day 8 after the induction of differentiation. (C) The stained Oil-Red O was eluted with 4% NP-40 in isopropanol and triglyceride content was quantified by measuring absorbance at 490 nm. The results are presented as the mean ± SD of three independent experiments. $^{###}p < 0.001$ indicates the significance compared to the vehicle-treated control. $^{***}p < 0.001$ indicates the significance compared to the MDI-treated control.

stained with hematoxylin and eosin and Oil-Red O staining. Considering the concentration used in the *in vitro* experiments, we expected to observe an effect at 15 mg/kg *in vivo* as well. As shown in Fig. 5A, the liver of the HFD group displayed typical signs of fatty liver showing the accumulation of lipid droplets throughout the liver. Conversely, much smaller and fewer lipid droplets were observed in the HFD with MCSC 15 mg/kg group. Hypertrophic adipocytes and hepatocytes in the HFD group were also attenuated by MCSC administration. Furthermore, histological analysis of the abdominal adipose tissues resulted in a smaller size of adipocytes in the MCSC-treated group compared to the HFD group (Fig. 5B), suggesting that the reduced body weight is mainly due to decreased fat accumulation in adipocytes. Additionally, we confirmed that MCSC modulates the protein expressions involved in lipid metabolism *in vivo*. As shown in Fig. 5C, the MCSC-treated group was significantly effective in reducing C/EBPα and PPARγ levels, both of which facilitate the decrease of lipogenesis in adipocyte differentiation. Given the potential for experimental results to translate into clinical applications, the fact that the drug shows efficacy at a lower dose, considering safety and side effects, could hold significant clinical importance.

To identify the anti-obesity compounds from MCSC, we evaluated the inhibitory effect of F1–F6 sub-fractions on adipocyte differentiation using an Oil-Red O staining assay. 3T3-L1 cells were differentiated with the MDI complex in the presence of each fraction for 8 days. Among the 6 fractions tested, the F4 fraction significantly decreased accumulated lipid contents compared to the control treated with the MDI complex in 3T3-L1 adipocytes. Subsequently, the F4 fraction was further fractionated into 15 fractions (F4.1–F4.15). Among these fractions, F4.3 was identified as the most potent fraction (Fig. 6). Therefore, the anti-adipogenic activity of the F4.3 fraction might be attributed to bioactive compounds. The F4.3 fraction was sub-fractionated using an MPLC set, and two compounds were putatively identified by QTOF/MS. The derivatives presented their *m/z* values at $[M+Na]^+$ 755 and $[M+Na]^+$ 739, respectively. Compound **1** was assigned the molecular formula $C_{42}H_{52}O_{11}Na$ based on its *m/z* 755.3345 $[M+Na]^+$ at positive-ion mode. To obtain spectrometric information specifically, it was used to select parent ions in MS^2 analysis. In the MS^2 spectra, the precursor produced ion fragments at *m/z* 559.2 and 409.2 (Supplementary Fig. 1A). Compound **2** was assigned the molecular formula $C_{41}H_{48}O_{11}Na$ based on its *m/z* 739.3152 $[M+Na]^+$ at positive-ion mode. In the MS^2 spectra, the precursor produced ion fragments at *m/z* 559.2 and 393.2 (Supplementary Fig. 1B). According to this spectrometric data, compound **1** and compound **2** were tentatively determined as manassantin A and manassantin B, respectively. We also confirmed the inhibitory effect of manassantin A and manassantin B on adipocyte differentiation. Compounds were used in a range of non-cytotoxic concentrations (2–50 nM). Both compounds significantly decreased accumulated lipid contents in a dose-dependent manner, compared to the control treated with the MDI complex in 3T3-L1 adipocytes (Fig. 6).

Our study expands on previous findings regarding the pharmacological properties of *S. chinensis*, providing new insights into its potential as an anti-obesity agent.[20] While previous reports have primarily focused on its antioxidant, anti-inflammatory, and cytotoxic properties of *S. chinensis* extract, our results

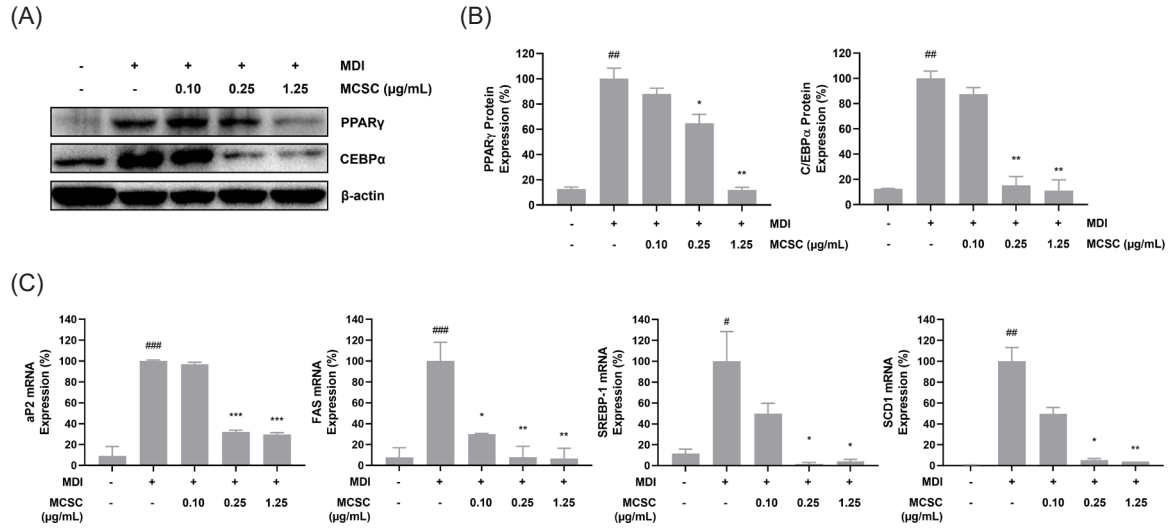

Fig. 3. Inhibitory effect of MCSC on C/EBPα and PPARγ expressions and adipogenic genes in 3T3-L1 cells. (A) The protein expression of C/EBPα and PPARγ levels in MCSC-treated 3T3-L1 adipocytes at day 6 of differentiation. (B) The bands were normalized to the β-actin signal. (C) The mRNA expression of aP2, FAS, SREBP-1, and SCD1, which are downstream of PPARγ and C/EBPα involved with the lipogenesis, in MCSC-treated 3T3-L1 adipocytes. The mRNA expressions were confirmed by qRT-PCR. The results are presented as the mean ± SD of three independent experiments. $^{\#}p < 0.05$, $^{\#\#}p < 0.01$, and $^{\#\#\#}p < 0.001$ indicate the significance compared to the vehicle-treated control. $*p < 0.05$, $**p < 0.01$, and $***p < 0.001$ indicate the significance compared to the MDI-treated control.

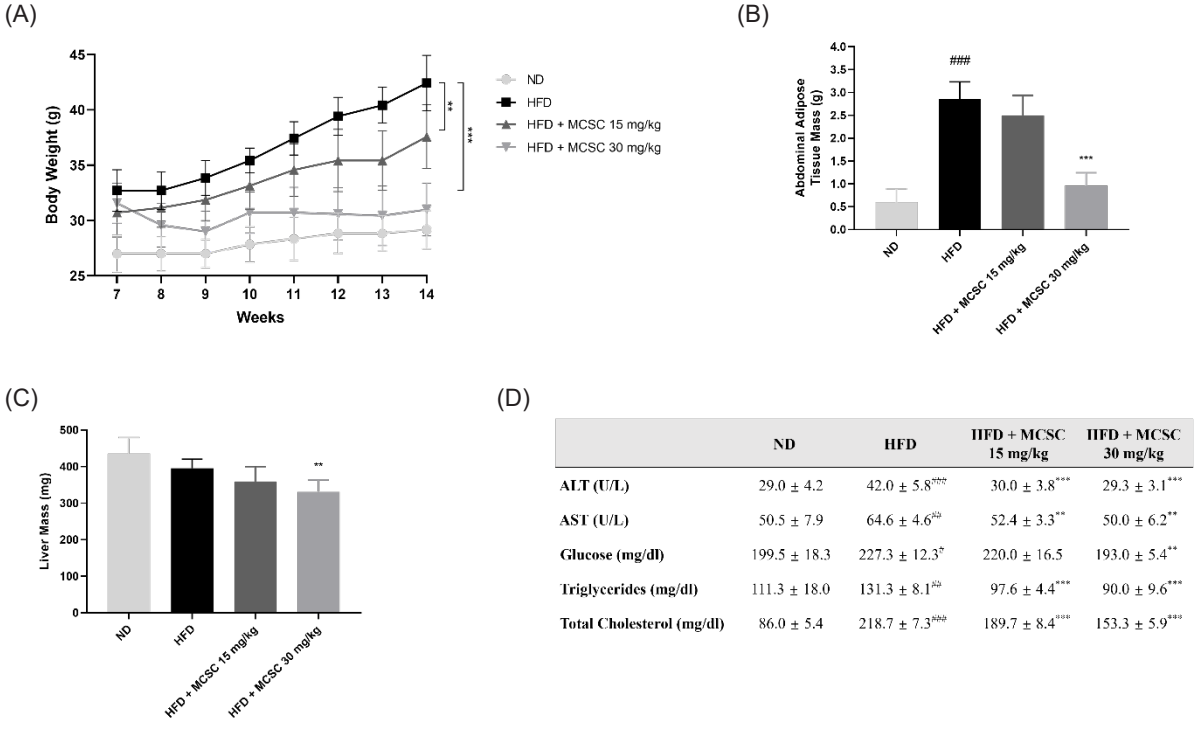

	ND	HFD	HFD + MCSC 15 mg/kg	HFD + MCSC 30 mg/kg
ALT (U/L)	29.0 ± 4.2	42.0 ± 5.8$^{\#\#\#}$	30.0 ± 3.8***	29.3 ± 3.1***
AST (U/L)	50.5 ± 7.9	64.6 ± 4.6$^{\#\#}$	52.4 ± 3.3**	50.0 ± 6.2**
Glucose (mg/dl)	199.5 ± 18.3	227.3 ± 12.3*	220.0 ± 16.5	193.0 ± 5.4**
Triglycerides (mg/dl)	111.3 ± 18.0	131.3 ± 8.1$^{\#\#}$	97.6 ± 4.4***	90.0 ± 9.6***
Total Cholesterol (mg/dl)	86.0 ± 5.4	218.7 ± 7.3$^{\#\#\#}$	189.7 ± 8.4***	153.3 ± 5.9***

Fig. 4. Inhibitory effect of MCSC on body weight gain and food intake in high-fat diet (HFD)-induced obese mice. (A) The effect of MCSC on body weight gain in mice. C57BL/6 mice were fed a normal diet and an HFD for 6 weeks. HFD-induced mice were orally administrated with MCSC (15 and 30 mg/kg) daily for 8 weeks. (B) The effect of MCSC on the weight of abdominal adipose tissue. (C) The effect of MCSC on the weight of liver. (D) The biochemical changes within serum. Alanine aminotransferase (ALT), aspartate aminotransferase (AST), triglycerides, total cholesterol, and glucose levels in the serum were measured using a commercial enzyme kit. $^{\#}p < 0.05$, $^{\#\#}p < 0.01$, and $^{\#\#\#}p < 0.001$ indicate the significance compared to the normal diet group. $**p < 0.01$ and $***p < 0.001$ indicate the significance compared to the HFD group.

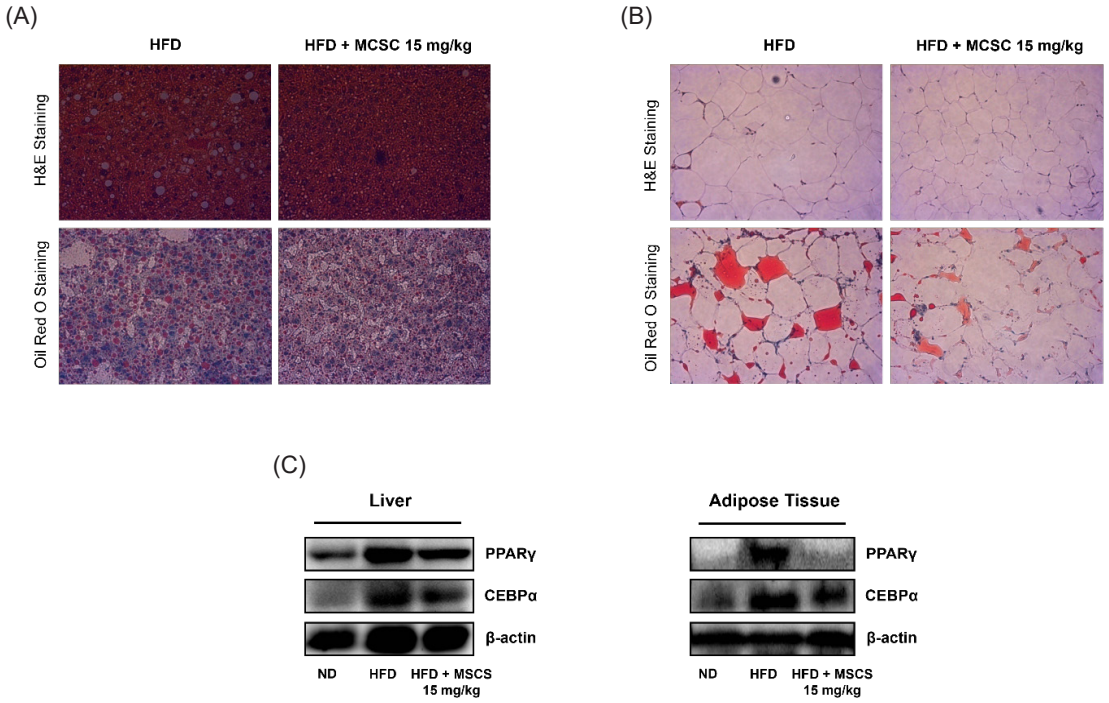

Fig. 5. Inhibitory effect of MCSC on the hepatic and abdominal fat accumulation. (A-B) Histological analysis of the liver in the HFD group was performed by hematoxylin and eosin (H&E) and Oil-Red O staining to confirm the accumulation of lipid droplets throughout the liver (A) and adipose tissue (B). Magnification: liver 400×, adipose tissue 200×. (C) The protein expressions of C/EBPα and PPARγ in liver and adipose tissue. The protein expressions were analyzed by western blotting.

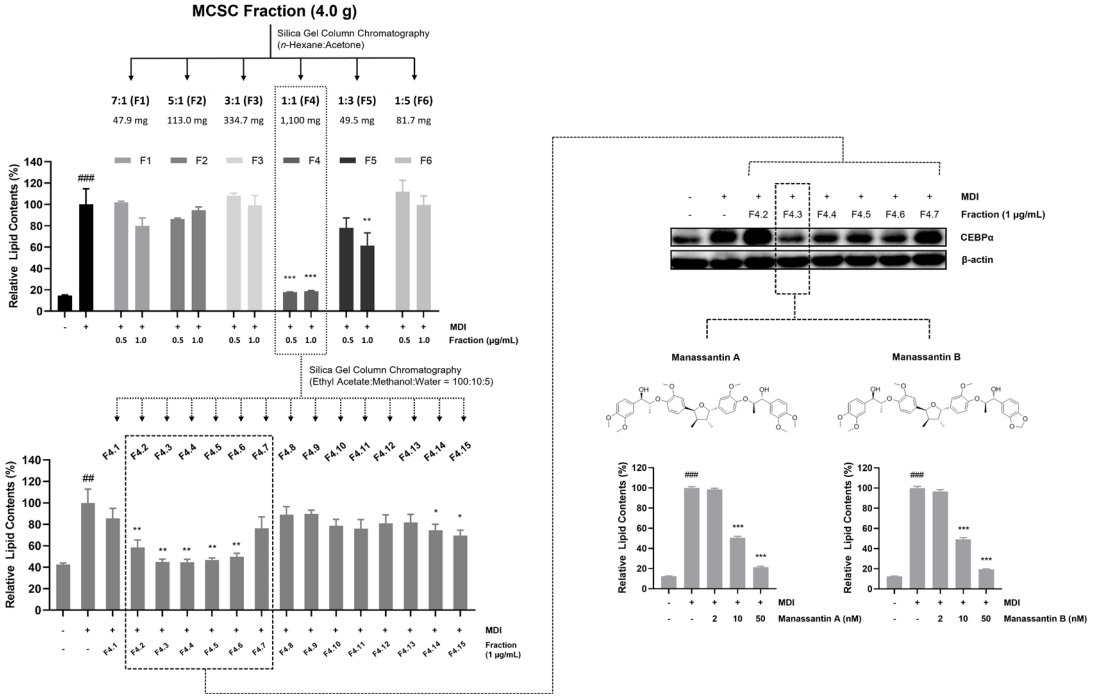

Fig. 6. Bioassay-guided fractionation of MCSC and their inhibitory effect on adipocyte differentiation. MCSC fraction was subjected to column chromatography to afford 6 fractions (F1–F6). F4 fraction was further fractionated to 15 fractions (F4.1–F4.15). 3T3-L1 cells were treated with fractions (0.5 or 1 μg/mL) and manassantin A and manassantin B (2, 10, and 50 nM). Lipid droplets accumulated in cells were stained with Oil-Red O on day 8 after the induction of differentiation. The protein expression of C/EBPα was confirmed by western blotting. $^{\#\#}p < 0.01$ and $^{\#\#\#}p < 0.001$ indicate the significance compared to the vehicle-treated control. $^{*}p < 0.05$, $^{**}p < 0.01$, and $^{***}p < 0.001$ indicate the significance compared to the MDI-treated control.

highlight active fraction of *S. chinensis* to inhibit adipogenesis and reduce obesity-related parameters. This novel application of *S. chinensis* adds valuable information to the existing literature on natural products for obesity management. The anti-adipogenic and anti-obesity effects of MCSC can be attributed to its active compounds, manassantin A and manassantin B, identified through HPLC and LC-ESI/MS analysis. Manassantin B is likely responsible for the inhibition of key adipogenic mediators and the resultant decrease in lipid accumulation.[24] By attenuating the expression of C/EBPα and PPARγ, these compounds disrupt the regulatory network essential for adipocyte differentiation and lipid storage. Despite the promising results, the precise molecular mechanisms through which MCSC exerts their effects need further elucidation. Additionally, long-term studies are necessary to assess the safety and efficacy of MCSC in humans. Investigating the bioavailability and pharmacokinetics of these active compounds will also be crucial for developing effective anti-obesity therapies.

In conclusion, MCSC from *S. chinensis* exhibits significant anti-adipogenic and anti-obesity effects by down-regulating key adipogenic transcription factors, leading to reduced body weight gain and improved lipid metabolism *in vitro* and *in vivo*. The active compounds, manassantin A and manassantin B, are identified as major contributors to these effects. These findings suggest that MCSC holds potential as a therapeutic agent for the prevention and treatment of obesity and its related metabolic disorders.

Acknowledgments

This work was supported by the National Research Foundation (NRF) of Korea (No. 2009-0083533 and 2020R1C1C1004573) funded by the Korean government.

Conflicts of Interest

The authors declare that they have no conflicts of interest.

References

(1) Williams, E. P.; Mesidor, M.; Winters, K.; Dubbert, P. M.; Wyatt, S. B. *Curr. Obes. Rep.* **2015**, *4*, 363–370.
(2) Dietrich, P.; Hellerbrand, C. *Best Pract. Res. Clin. Gastroenterol.* **2014**, *28*, 637–653.
(3) Martel, J.; Ojcius, D. M.; Chang, C.-J.; Lin, C.-S.; Lu, C.-C.; Ko, Y.-F.; Tseng, S.-F.; Lai, H.-C.; Young, J. D. *Nat. Rev. Endocrinol.* **2017**, *13*, 149–160.
(4) Tucci, S. A.; Boyland, E. J.; Halford, J. C. *Diabetes Metab. Syndr. Obes.* **2010**, *3*, 125–143.
(5) Suzuki, K.; Jayasena, C. N.; Bloom, S. R. *Exp. Diabetes Res.* **2012**, *2012*, 824305.
(6) Ghaben, A. L.; Scherer, P. E. *Nat. Rev. Mol. Cell Biol.* **2019**, *20*, 242–258.
(7) Vishvanath, L.; Gupta, R. K. *J. Clin. Invest.* **2019**, *129*, 4022–4031.
(8) Hausman, D. B.; DiGirolamo, M.; Bartness, T. J.; Hausman, G. J.; Martin, R. J. *Obes. Rev.* **2001**, *2*, 239–254.
(9) Sun, K.; Kusminski, C. M.; Scherer, P. E. *J. Clin. Invest.* **2011**, *121*, 2094–2101.
(10) Chaiittianan, R.; Sutthanut, K.; Rattanathongkom, A. *J. Ethnopharmacol.* **2017**, *201*, 9–16.
(11) Tsui, L. *SLAS Discov.* **2022**, *27*, 375–383.
(12) Madsen, M. S.; Siersbæk, R.; Boergesen, M.; Nielsen, R.; Mandrup, S. *Mol. Cell. Biol.* **2014**, *34*, 939–954.
(13) Moseti, D.; Regassa, A.; Kim, W.-K. *Int. J. Mol. Sci.* **2016**, *17*, 124.
(14) Jin, Q.; Lee, J. W.; Kim, J. G.; Lee, D.; Hong, J. T.; Kim, Y.; Lee, M. K.; Hwang, B. Y. *J. Nat. Prod.* **2019**, *82*, 3002–3009.
(15) Yoo, H.-J.; Kang, H.-J.; Jung, H.-J.; Kim, K.; Lim, C.-J.; Park, E.-H. *J. Ethnopharmacol.* **2008**, *120*, 282–286.
(16) Zhang, J.; Rho, Y.; Kim, M.-Y.; Cho, J. Y. *J. Ethnopharmacol.* **2021**, *279*, 114400.
(17) Yu, M. H.; Im, H. G.; Lee, J.-W.; Hwang Bo, M.-H.; Kim, H.-J.; Kim, S. K.; Chung, S. K.; Lee, I.-S. *Nat. Prod. Res.* **2008**, *22*, 275–283.
(18) Meng, X.; Kim, I.; Jeong, Y. J.; Cho, Y. M.; Kang, S. C. *Exp. Biol. Med. (Maywood)* **2016**, *241*, 396–408.
(19) Jeong, H. J.; Koo, B.-S.; Kang, T.-H.; Shin, H. M.; Jung, S.; Jeon, S. *Phytomedicine* **2015**, *22*, 256–261.
(20) Shin, O.-S.; Shin, Y.-H.; Lee, K.-H.; Kim, G.-Y.; Kim, K.-H.; Park, J.-K.; Ahn, J.-I.; Song, K.-Y. *KSBB Journal* **2012**, *27*, 381–386.
(21) Wang, L.; Cheng, D.; Wang, H.; Di, L.; Zhou, X.; Xu, T.; Yang, X.; Liu, Y. *J. Ethnopharmacol.* **2009**, *126*, 487–491.
(22) Hwang, J.-Y.; Zhang, J.; Kang, M.-J.; Lee, S.-K.; Kim, H.-A.; Kim, J.-J.; Kim, J.-I. *Nutr. Res. Pract.* **2007**, *1*, 100–104.
(23) Hishida, T.; Nishizuka, M.; Osada, S.; Imagawa, M. *Biochimie* **2009**, *91*, 654–657.
(24) Cai, J.; Qiong, G.; Li, C.; Sun, L.; Luo, Y.; Yuan, S.; Gonzalez, F. J.; Xu, J. *FASEB J.* **2021**, *35*, e21496.

Received July 25, 2024
Revised September 13, 2024
Accepted September 13, 2024